Research Article | Vol. 30, No. 12 / 6 Jun 2022 / Optics Express 21386
Optics EXPRESS

Full-space omnidirectional cloak by subwavelength metal channels filled with homogeneous dielectrics

BO WANG,[1,3] FEI SUN,[1,3,*] HANCHUAN CHEN,[1] YICHAO LIU,[1] YUAN LIU,[2] AND XIN LIU[1]

[1] *Key Lab of Advanced Transducers and Intelligent Control System, Ministry of Education and Shanxi Province, College of Physics and Optoelectronics, Taiyuan University of Technology, Taiyuan 030024, China*
[2] *High-Tech Institute of Xi'an, Shaanxi, Xi'an 710025, China*
[3] *Equal contributors.*
[*] *sunfei@tyut.edu.cn*

Abstract: Cloaks can greatly reduce the scattering cross-section of hidden objects through various mechanisms, thereby making them invisible to outside observers. Among them, the full-space omnidirectional cloak based on transformation optic with full parameters are difficult to realize without metamaterials and often needs to be simplified before realization, while most cloaks with simplified parameters have limited working direction and cannot achieve omnidirectional cloaking effect. In this study, a full-space omnidirectional cloak is designed based on transformation optics and optic-null medium, which only needed natural materials without metamaterials. The designed omnidirectional cloak is realized by subwavelength metal channels filled with isotropic dielectrics whose refractive indices range from 1 to 2, which is homogeneous in each channel. The numerical simulation results verify good scattering suppression effect of the designed cloak for various detecting waves.

1. Introduction

The perfect electromagnetic cloak can create a concealed region that is invisible (i.e., scattering cross-section is zero) for arbitrary detecting waves, which can be designed by various methods [1–3]. Among these methods, transformation optic (TO), which is based on the form-invariance of Maxwell's equations under coordinate transformations, is the most common way used to design perfect cloaks [4–6]. However, the full parameters of perfect cloak, which is often inhomogeneous anisotropic medium with singularity, are difficult to realize without reductions. To realize the function of invisibility, various methods have been proposed to reduce the parameters of the perfect cloak, which include eikonal approximation [7–9], line-extended transformation [10–12], triangular transformations in blocks [13–15], sacrificing phase information or directions of observation [16–20], designing together with deep learning or optimization algorithms [21–24], introducing optic-null medium (ONM) [25–30] and metasurfaces [31–34]. Most previous cloaks require the use of metamaterials (usually involving sub-wavelength processing techniques and gradual control of unit's geometrical parameters) [7–15], and very few cloaks have been achieved by natural materials (without artificial structures) [16–18,25–27]. However, these cloaks by natural materials cannot achieve omnidirectional invisible effect (only effective for a few discrete detecting directions or a certain range of incidence angles). Note that most of the current experimentally validated cloaks are carpet cloaks (half-space invisibility) [35–39], which can make a curved surface appear to be a flat plane rather than reducing the scattering cross-section as full-space cloaks. The common problem with current full-space cloaks is that they either require the need of metamaterials to realize, or are only effective for a limited number

#460395 https://doi.org/10.1364/OE.460395
Journal © 2022 Received 5 Apr 2022; revised 10 May 2022; accepted 16 May 2022; published 31 May 2022

Optics EXPRESS

of detecting directions. It is still challenging to realize omnidirectional invisibility cloak with natural materials.

ONM is an extremely high anisotropic medium derived from TO, and can be utilized to design various electromagnetic devices that previously could only be designed by TO [40–45]. In recent years, many full-space cloaks with easily achievable parameters have been proposed and experimentally verified with the help of ONM [25–30]. However, the current full-space cloaks based on ONM still have the problems described above, i.e., they either have restricted detecting directions [26,27] or require the use of metamaterials to realize [29,30]. In this study, we design full-space omnidirectional cloak with easily achievable parameters by natural materials that can greatly reduce the scattering cross-section. Firstly, an omnidirectional cloak is designed by TO, and then OMN is introduced to simplify the parameters of the designed cloak. Then, subwavelength metal channels surrounded by metal plates and filled with homogeneous isotropic dielectric in each channel are designed to realize the designed omnidirectional cloak.

As shown in Fig. 1(a), the designed cloak is made up of subwavelength metal channels filled with homogeneous isotropic dielectric in each channel. The subwavelength metal channels are surrounded by metal plates, which are designed as linear segments and modeled as perfect electric conductors in microwave frequencies. The refractive indices in each channel are homogeneous, which are between 1 and 2 (see Fig. 1(b)). The concealed regions are located in the four corners of the cloak, within which objects of any shape and material can be hidden for detecting waves from any direction.

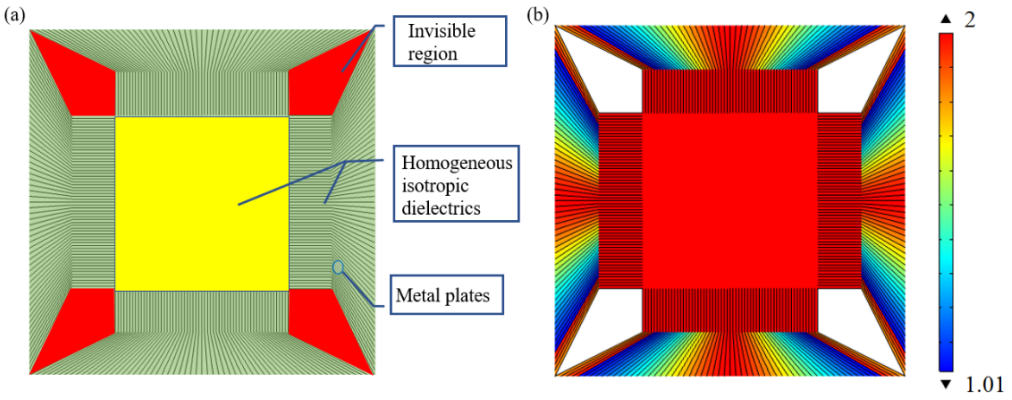

Fig. 1. (a) The schematic diagram of the designed full-space omnidirectional cloak by metal plates (thick black lines) and dielectrics (colored green and yellow). The concealed region is indicated by four red quadrilaterals, which are enclosed by metal plates. (b) The refractive indices distribution within the cloak in (a). The refractive indices of the objects inside the concealed region (colored white) can be arbitrary.

2. Omnidirectional cloak by TO and ONM

The coordinate transformation used to design omnidirectional cloak is shown in Fig. 2. The identity transformation is used on the exterior of two square areas with side length l_3. The correspondence between various regions within the two square areas with side length l_3 are: the thin green region in the reference space is stretched to the thick green region in the real space; the yellow square region with length l_2 in the reference space is compressed to the yellow square region with length l_1 in the real space; the short line segments (colored thick black) at four corners in the reference space are expanded to four polygonal areas (colored gray) in the real space. From the perspective of TO, the scattering cross section of concealed regions (i.e., four

Optics EXPRESS

gray polygonal areas) in the real space is the same as the scattering cross section of four short line segments in the reference space, which can greatly reduce the scattering of the concealed objects. Furthermore, the four short line segments in the reference space can also be designed as four points when their lengths approach to zero, which can be obtained by introducing ONM later, and in this case perfect omnidirectional invisibility can be created.

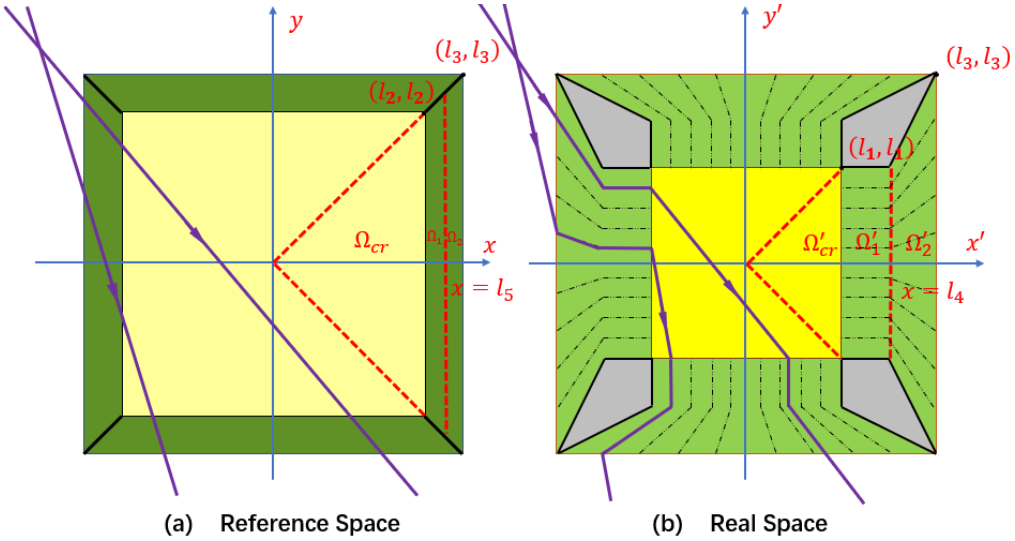

Fig. 2. The correspondence between different regions between (a) the reference space and (b) the real space to design an omnidirectional cloak. The green region and yellow region are stretched and compressed respectively from the reference space to the real space. The gray regions are concealed region. The purple lines represent two corresponding light trajectories with different incident angles. In reference space, the right-angled triangular region in the first and fourth quadrants can be divided into three regions Ω_1, Ω_2 and Ω_{cr} (we choose $l_4 = (l_1 + l_3)/2$ and $l_5 = (l_2 + l_3)/2$ in our design), which correspond to Ω_1', Ω_2' and Ω_{cr}' in real space.

Two square areas with side length l_3 in Fig. 2 can be divided into four right-angled triangular regions based on their diagonals. Take the example of right-angled triangular region in the first and fourth quadrants, the coordinate transformation in Fig. 2 can be expressed as:

$$\begin{cases} x' = \begin{cases} l_1 x / l_2, (x, y) \in \Omega_{cr} \\ K_1 x + C_1, (x, y) \in \Omega_1 \\ K_2 x + C_2, (x, y) \in \Omega_2 \end{cases} \\ y' = \begin{cases} l_1 y / l_2, (x, y) \in \Omega_{cr} \\ l_1 y / x, (x, y) \in \Omega_1 \\ (K_3 x + C_3) y / x, (x, y) \in \Omega_2 \end{cases} \\ z' = z \end{cases}, \tag{1}$$

where $K_1 = (l_4\text{-}l_1)/(l_5\text{-}l_2)$, $C_1 = l_4\text{-}K_1 l_5$, $K_2 = (l_3\text{-}l_4)/(l_3\text{-}l_5)$, $C_2 = l_4\text{-}K_2 l_5$, $K_3 = (l_3\text{-}l_1)/(l_3\text{-}l_4)$, and $C_3 = l_1\text{-}K_3 l_4$ are constants related to the internal geometry of two square areas. The quantities

Optics EXPRESS

with and without primes are used to represent quantities in real space and reference space, respectively. Identity transformation is used on the exterior of two square areas, therefore the exterior of both square areas is air. Based on symmetry, the coordinate transformations in other right-angled triangular regions can be obtained by taking the replacement in Eq. (1): $(x, y)\rightarrow(y, x)$, $(x', y')\rightarrow(y', x')$ for the triangular regions in the first and second quadrants; $(x, y)\rightarrow(-y, x)$, $(x', y')\rightarrow(-y', x')$ for the triangular regions in the third and fourth quadrants; $(x, y)\rightarrow(-x, y)$, $(x', y')\rightarrow(-x', y')$ for the triangular regions in the second and third quadrants.

The corresponding relationship between permittivity/permeability in the reference space and the real space can be calculated by TO [4–6]:

$$\begin{cases} \varepsilon' = \frac{J\varepsilon J^T}{\det(J)} \\ \mu' = \frac{J\mu J^T}{\det(J)} \end{cases}, \tag{2}$$

where the $J=\partial(x', y', z')/\partial(x, y, z)$ is Jacobian matrix whose determinant is $\det(J)$. The permittivity and permeability of the designed cloak in the real space can be obtained by using Eq. (1) and Eq. (2):

$$\varepsilon' = \mu' = \begin{cases} diag(1, 1, (l_2/l_1)^2), (x', y') \in \Omega'_{cr} \\ \begin{pmatrix} a_{11} & a_{12} & 0 \\ a_{21} & a_{22} & 0 \\ 0 & 0 & a33 \end{pmatrix}, (x', y') \in \Omega'_1 \\ \begin{pmatrix} b_{11} & b_{12} & 0 \\ b_{21} & b_{22} & 0 \\ 0 & 0 & b33 \end{pmatrix}, (x', y') \in \Omega'_2 \end{cases}, \tag{3}$$

where

$$\begin{cases} a_{11} = (-C_1 + x')/l_1 \\ a_{12} = a_{21} = -(y'/l_1) \\ a_{22} = -((l_1{}^2 + y'^2)/(C_1 l_1 - l_1 x')) \\ a_{33} = (-C_1 + x')/(K_1{}^2 l_1) \\ b_{11} = K_2(-C_2 + x')/D(x') \\ b_{12} = b_{21} = -C_3 K_2{}^2 y'/D^2(x')\text{‘} \\ b_{22} = K_2{}^3[(D(x')/K_2)^4 + C_3{}^2 y'^2\,]/[\,(x' - C_2)D^3(x')] \\ b_{33} = (-C_2 + x')/(K_2 D(x')) \end{cases}. \tag{4}$$

The permittivity and permeability of the designed cloak in regions Ω_1 and Ω_2 can also be expressed as diagonal matrices through coordinate rotation in its principal axis coordinate system. In this case, the permittivity and permeability of the designed cloak in Eq. (3) can be further expressed as:

$$\varepsilon'_d = \mu'_d = \begin{cases} diag(1, 1, (l_2/l_1)^2), (x', y') \in \Omega'_{cr} \\ diag(\frac{1}{2}\left(a_{11} + a_{22} + \sqrt{P}\right), \frac{1}{2}\left(a_{11} + a_{22} - \sqrt{P}\right), a_{33}), (x', y') \in \Omega'_1 \\ diag(\frac{1}{2}\left(b_{11} + b_{22} + \sqrt{Q}\right), \frac{1}{2}\left(b_{11} + b_{22} - \sqrt{Q}\right), b_{33}), (x', y') \in \Omega'_2 \end{cases}, \tag{5}$$

Optics EXPRESS

where $P = a_{11}{}^2+4a_{12}{}^2-2a_{11}a_{22}+a_{22}{}^2$ and $Q = b_{11}{}^2+4b_{12}{}^2-2b_{11}b_{22}+b_{22}{}^2$. The subscript '$d$' in Eq. (5) indicates that the permittivity and permeability are diagonalized in the principal axis coordinate system. Note that the designed cloak in Eq. (5) has two limitations: the first is that the designed cloak is gradient as parameters in Eq. (5) which are related with x' and y'. Secondly, the cloaking effect is not perfect, as the gray concealed regions in the real space correspond to the short black segments of certain length (not ideal points without cross-sections) in the reference space. Only if these line segments in the reference space are much smaller than the detecting wavelength, the designed cloak can give a good performance. Next, we will show how to eliminate material gradient and create a perfect invisibility by introducing ONM.

If the green region in Fig. 2(a) is extremely thin (i.e., $l_3 \to l_2$), it will be reduced to a surface (will no longer be a volume of space), and the short black segments will be reduced to points. In this case, the gray regions in the real space are compressed into points in the reference space, the perfect invisibility can be expected. At the same time, ideal ONM are introduced in the green region in the real space (corresponds to the surface in the reference space). This can be made by taking the limitation $l_2 \to l_3$ in Eq. (5):

$$\varepsilon'_d = \mu'_d = \begin{cases} diag(1,1,(\frac{l_2}{l_1})^2),(x',y') \in \Omega'_{cr} \\ diag(\frac{2l_1}{\Delta},\frac{\Delta}{4l_1},\frac{2\Delta}{l_1}) \overset{\Delta=l_3-l_2\to 0}{\longrightarrow} diag(\infty,0,0),(x',y') \in \Omega'_1 \\ diag(\frac{l_1}{\Delta},\frac{\Delta}{l_1},\frac{\Delta}{l_1}) \overset{\Delta=l_3-l_2\to 0}{\longrightarrow} diag(\infty,0,0),(x',y') \in \Omega'_2 \end{cases}, \tag{6}$$

with $\Delta = l_3 - l_2 \to 0$. By assuming $l_2 \to l_3$, the media in the regions in Ω_1' and Ω_2' are ideal ONM. Numerical simulations in Fig. 3 verify the omnidirectional cloaking effect of the designed cloak based on ideal ONM in Eq. (6). As shown in Fig. 3, four concealed regions (modeled as perfect

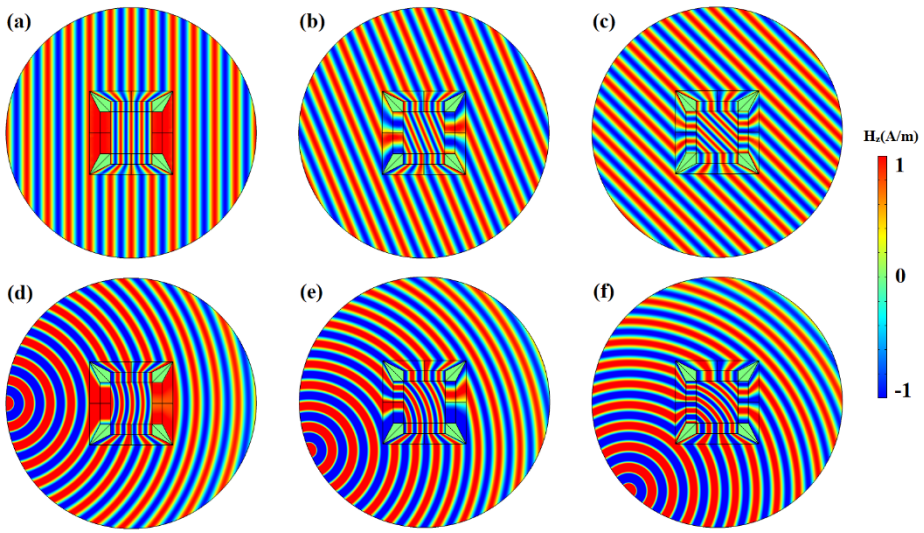

Fig. 3. The simulated normalized magnetic field's z component H_z for the omnidirectional cloak with Eq. (6) when the detecting source is a plane wave (a)~(c) or a line current (d)~(f). (a)~(c) The detecting plane waves are incident on the cloak from 0 degree (a), 22.5 degrees (b), and 45 degrees (c). (d)~(f) The detecting line currents are located at (a) (-6λ, 0), (b) (-5.54λ, -2.30λ), and (c) (-4.24λ, -4.24λ) from the center of the cloak. The simulation domain is surrounded by perfect matched layer with a thickness of λ/10. The geometrical parameters of the designed cloak are chosen as $l_1 = \lambda$, $l_2 = 1.99\lambda$, $l_3 = 2\lambda$, $l_4 = (l_1 + l_3)/2$, $l_5 = (l_2 + l_3)/2$, and λ=1 cm.

Optics EXPRESS

electric conductor (PEC) in simulations) have no scattering effect on plane waves incident from different directions or on line current radiation at different spatial locations, thus verifying the omnidirectional working characteristics of the designed cloak.

3. Realization design

The permittivity and permeability of the ideal ONM, which is infinite large along its main axis and zero in other directions, is almost impossible to achieve. However, there have been some implementations and experimental validations of reduced ONM [25–30,40,41]. These methods of implementing reduced ONM can be classified into two main categories: one is based on metamaterials (which usually operate near the cut-off frequency of the waveguide metamaterial) [29,30,41], and the other is based on subwavelength metal channels [25–28,40]. Compared with metamaterials, metal channels are easier to process (without fabricating subwavelength artificial units). Previous cloaks, which are based on ONM implemented with metal channels, have equal length between input and output surfaces [26,27,29]. Although they can be realized by equal length metal plates without filling any media (i.e., air channels), these cloaks are only effective for a limited number of detecting directions. To achieve omnidirectional cloak by metal channels, metal plates of equal length cannot be used, which would result in having to fill each metal channel with some dielectrics. Different from previous methods (i.e., each channel is filled with a graded refractive index medium) [28], our design is to fill each metal channel with a homogeneous dielectric to achieve omnidirectional cloaking effect.

To realize the ONM in the regions Ω1' and Ω2' (see Eq. (6)), we can fill homogeneous dielectrics in subwavelength metal channels (see Fig. 1(a)). The metal channels are surrounded by metal plates, whose orientations are consistent with the main axes of ONM and separations are between $\lambda/15$ and $\lambda/30$ in our design. Since the geometry of the designed cloak are symmetric about the center of the origin, we only give the design of the metal channels and filling materials in the first quadrant. The channels in the first quadrant are marked with the channel number p in Fig. 4(a), which is a positive integer and ranges from 1 to 30. The refractive indices n_p of the p-th metal channel can be designed according to the following FP condition:

$$\int_{l_p} n_p dl = \frac{m\lambda}{2}, \tag{7}$$

where l_p is the geometrical length of the p-th channel and m is a positive integer, which are related with the channel number p in Fig. 4(b). The metal channels and the filling materials in other quadrants can be designed by rotating the design in the first quadrant around the origin (see Fig. 1(b)). The cloaking effect can be further improved by increasing the total channel number (i.e., reducing the separation between each metal channel), as the larger total channel number can make the effective parameters of the channel structure closer to the perfect ONM. However, the larger total channel number will increase the difficulty of fabricating the structure.

Numerical simulations verify the designed cloak by subwavelength metal channels filled with homogeneous dielectric in Fig. 1 can greatly reduce scattering when the detecting plane wave incidents from different angles (see Fig. 5(a)-(c)). For comparison, Figs. 5(d)-(f) show the cases that the designed cloak is removed (only four PEC corners are left) when the detecting plane wave incidents from corresponding angles, in which obvious scattering appear. To further verify the omnidirectional cloaking effect of the designed metal channel structure, the detecting source is chosen as a line current in Fig. 6. When the detecting line current is located at different positions, the four PEC quadrangles in free space will produce noticeable scattering (see Fig. 6(d)-(f)). Once the designed cloak by metal channels is applied around four PEC quadrangles, the scattering can be greatly reduced (see Fig. 6(a)-(c)).

As homogeneous dielectrics are filled inside subwavelength metal channels in Fig. 4, it will cause a sharp change in the refractive index at the boundary between the channels and the

Optics EXPRESS

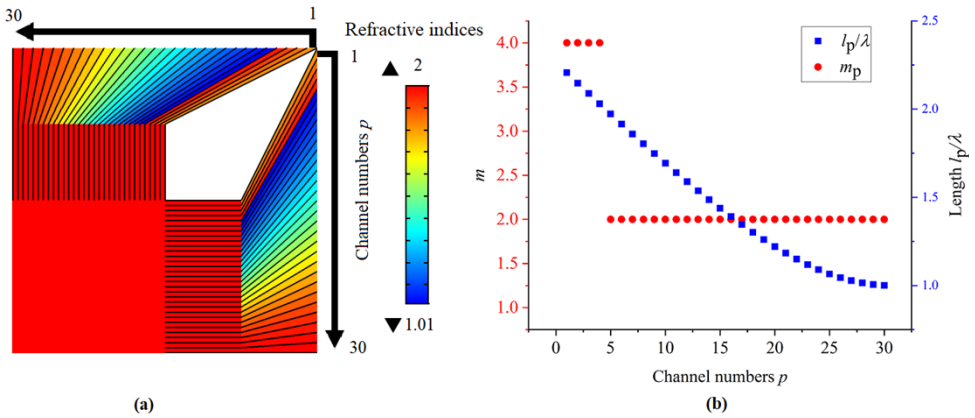

Fig. 4. (a) Adjacent metal plates (black lines) form a channel. The channel numbers p from 1 to 30 start from the tail of the arrow and increase in the direction of the arrow. (b) Relative length L_p/λ and the integer multiple number m_p of each subwavelength channel (only shows subwavelength channels of the region Ω_1' and Ω_2' due to symmetry).

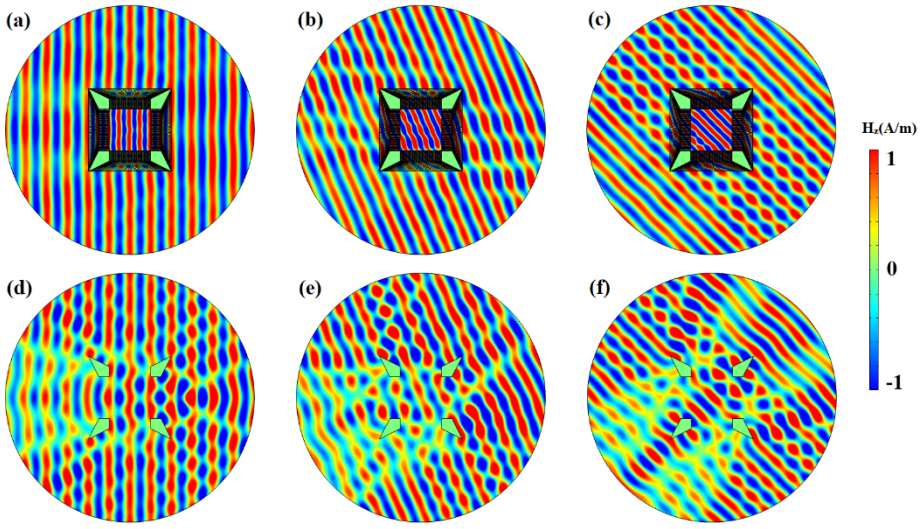

Fig. 5. The simulated normalized magnetic field's z component H_z when the detecting plane wave incident onto four PEC quadrangles with the designed cloak by metal channels (a)-(c) and without the designed cloak (d)-(f). The detecting plane waves incident from 0 degree (a), (d), 22.5 degrees (b), (e), and 45 degrees (c), (f).

Optics EXPRESS

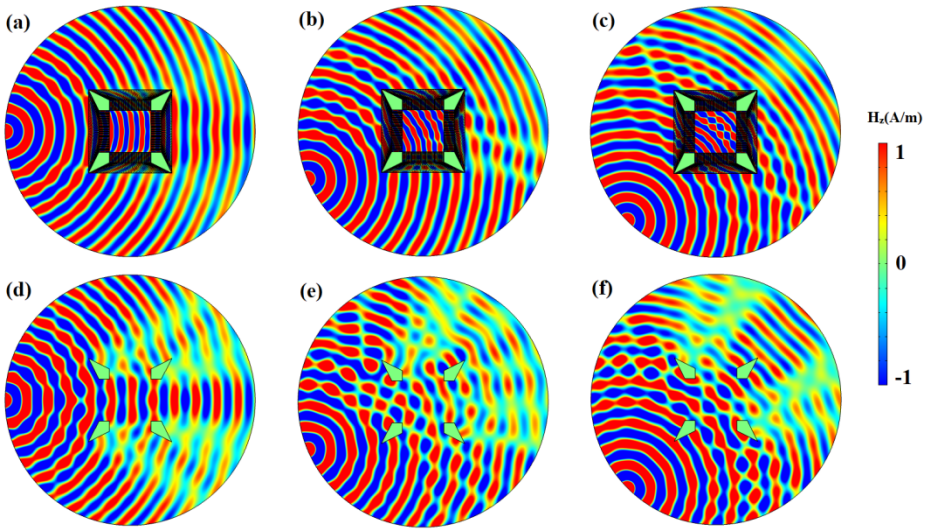

Fig. 6. The simulated normalized magnetic field's z component H_z when the detecting source is a line current. (a)-(c) the four PEC quadrangles are inside the designed cloak by metal channels. (d)-(f) the four PEC quadrangles are in free space without the designed cloak. The detecting line currents are located at (-6λ, 0) for (a) and (d), (-5.54λ, -2.30λ) for (b) and (e) and (-4.24λ, -4.24λ) for (c) and (f) from the center of the four PEC quadrangles.

air/center regions, which leads to the impedance mismatch and results in weak scatterings in Figs. 5(a)-(c) and Figs. 6(a)-(c). These weak scatterings can be reduced by using dielectrics with gradient refractive index to fill each metal channel. However, it would be very difficult to fabricate the channels with inhomogeneous materials.

A similar structure has been designed by other group [28], which numerically shows a good cloaking effect for detecting beam with a finite width. Compared with the cloak in Ref. 28, our design in Fig. 3 has a better performance, i.e., the average radar cross sections (RCS) for detected waves of different incident directions are $6.76\times10^{-4}\lambda$ for the cloak in Ref. 28 and $4.33\times10^{-8}\lambda$ for our cloak in Fig. 3, respectively. In addition, the proposed omnidirectional cloak in Fig. 3 can be realized by natural materials in Fig. 1 without metamaterials.

4. Conclusions

The current full-space cloaks based on TO either have restricted detecting directions or require the use of metamaterials to realize. To achieve omnidirectional invisibility effect without metamaterials, a full-space omnidirectional cloak that can greatly reduce the scattering cross-section of hidden objects for detecting waves from any direction by natural materials is proposed by TO and ONM. The proposed cloak can be realized by subwavelength metal channels filled with homogeneous isotropic dielectrics in each channel, which shows good omnidirectional scattering reduction effect from various detecting waves. Compared with previous invisibility cloaks, the designed cloak in this study can not only be effective for the detecting wave from any direction, but also only need metal plates and homogeneous dielectrics with refractive indices between 1 and 2, which provides an effective and simple way to achieve omnidirectional cloak without metamaterial.

Funding. National Natural Science Foundation of China (61971300, 61905208).

Disclosures. The authors declare no conflicts of interest.

Optics EXPRESS

Data availability. Data underlying the results presented in this paper are not publicly available at this time but may be obtained from the authors upon reasonable request.

References

1. P. Alitalo and S. Tretyakov, "Electromagnetic cloaking with metamaterials," Mater. Today **12**(3), 22–29 (2009).
2. A. V. Shchelokova, I. V. Melchakova, A. P. Slobozhanyuk, E. A. Yankovskaya, C. R. Simovski, and P. A. Belov, "Experimental realization of invisibility cloaking," Phys.-Usp. **58**(2), 167–190 (2015).
3. C. Qian and H. Chen, "A perspective on the next generation of invisibility cloaks-Intelligent cloaks," Appl. Phys. Lett. **118**(18), 180501 (2021).
4. J. B. Pendry, "Controlling Electromagnetic Fields," Science **312**(5781), 1780–1782 (2006).
5. F. Sun, B. Zheng, H. Chen, W. Jiang, S. Guo, Y. Liu, Y. Ma, and S. He, "Transformation Optics: From Classic Theory and Applications to its New Branches," Laser Photonics Rev. **11**(6), 1700034 (2017).
6. H. Chen, C. T. Chan, and P. Sheng, "Transformation optics and metamaterials," Nat. Mater. **9**(5), 387–396 (2010).
7. D. Schurig, J. J. Mock, B. J. Justice, S. A. Cummer, J. B. Pendry, A. F. Starr, and D. R. Smith, "Metamaterial Electromagnetic Cloak at Microwave Frequencies," Science **314**(5801), 977–980 (2006).
8. W. Cai, U. K. Chettiar, A. V. Kildishev, and V. M. Shalaev, "Optical cloaking with metamaterials," Nat. Photonics **1**(4), 224–227 (2007).
9. B. Kanté, D. Germain, and A. de Lustrac, "Experimental demonstration of a nonmagnetic metamaterial cloak at microwave frequencies," Phys. Rev. B **80**(20), 201104 (2009).
10. W. X. Jiang, H. Feng Ma, Q. Cheng, and T. J. Cui, "A class of line-transformed cloaks with easily realizable constitutive parameters," J. Appl. Phys. **107**(3), 034911 (2010).
11. Y. Luo, J. Zhang, H. Chen, L. Ran, B. I. Wu, and A. K. Jin, "A Rigorous Analysis of Plane-Transformed Invisibility Cloaks," IEEE Trans. Antennas Propag. **57**(12), 3926–3933 (2009).
12. N. Landy and D. R. Smith, "A full-parameter unidirectional metamaterial cloak for microwaves," Nat. Mater. **12**(1), 25–28 (2013).
13. T. Han, C. Qiu, and X. Tang, "An arbitrarily shaped cloak with nonsingular and homogeneous parameters designed using a twofold transformation," J. Opt. **12**(9), 095103 (2010).
14. W. Li, J. Guan, Z. Sun, W. Wang, and Q. Zhang, "A near-perfect invisibility cloak constructed with homogeneous materials," Opt. Express **17**(26), 23410–23416 (2009).
15. G. Zhu, "Designing a square invisibility cloak using metamaterials made of stacked positive-negative index slabs," J. Appl. Phys. **113**(16), 163103 (2013).
16. B. Zheng, R. Zhu, L. Jing, Y. Yang, L. Shen, H. Wang, Z. Wang, X. Zhang, X. Liu, E. Li, and H. Chen, "3D Visible-Light Invisibility Cloak," Adv. Sci. **5**(6), 1800056 (2018).
17. H. Chen and B. Zheng, "Broadband polygonal invisibility cloak for visible light," Sci. Rep. **2**(1), 255 (2012).
18. H. Chen, B. Zheng, L. Shen, H. Wang, X. Zhang, N. I. Zheludev, and B. Zhang, "Ray-optics cloaking devices for large objects in incoherent natural light," Nat. Commun. **4**(1), 2652 (2013).
19. Z. Zhen, C. Qian, Y. Jia, Z. Fan, R. Hao, T. Cai, B. Zheng, H. Chen, and E. Li, "Realizing transmitted metasurface cloak by a tandem neural network," Photonics Res. **9**(5), B229–B235 (2021).
20. H. Chu, Q. Li, B. Liu, J. Luo, S. Sun, Z. H. Hang, L. Zhou, and Y. Lai, "A hybrid invisibility cloak based on integration of transparent metasurfaces and zero-index materials," Light: Sci. Appl. **7**(1), 50 (2018).
21. B.-I. Popa and S. A. Cummer, "Cloaking with optimized homogeneous anisotropic layers," Phys. Rev. A **79**(2), 023806 (2009).
22. S. Xu, X. Cheng, S. Xi, R. Zhang, H. O. Moser, Z. Shen, Y. Xu, Z. Huang, X. Zhang, F. Yu, B. Zhang, and H. Chen, "Experimental Demonstration of a Free-Space Cylindrical Cloak without Superluminal Propagation," Phys. Rev. Lett. **109**(22), 223903 (2012).
23. L. Lan, F. Sun, Y. Liu, C. K. Ong, and Y. Ma, "Experimentally demonstrated a unidirectional electromagnetic cloak designed by topology optimization," Appl. Phys. Lett. **103**(12), 121113 (2013).
24. A. Mirzaei, A. E. Miroshnichenko, I. V. Shadrivov, and Y. S. Kivshar, "All-Dielectric Multilayer Cylindrical Structures for Invisibility Cloaking," Sci. Rep. **5**(1), 9574 (2015).
25. Z. Wang, Y. Liu, T. Cheng, F. Sun, and S. He, "Designing conformal cloaks by manipulating structures directly in the physical space," Opt. Express **28**(16), 23105–23113 (2020).
26. F. Sun, Y. Zhang, J. Evans, and S. He, "A camouflage device without metamaterials," Prog. Electromagn. Res. **165**, 107–117 (2019).
27. F. Sun, Y. Liu, and S. He, "Surface transformation multi-physics for controlling electromagnetic and acoustic waves simultaneously," Opt. Express **28**(1), 94–106 (2020).
28. L. Xu, Q. Wu, Y. Zhou, and H. Chen, "Transformation devices with optical nihility media and reduced realizations," Front. Phys. **14**(4), 42501 (2019).
29. Y. Zhang, Y. Luo, J. B. Pendry, and B. Zhang, "Transformation-Invariant Metamaterials," Phys. Rev. Lett. **123**(6), 067701 (2019).
30. B. Zheng, Y. Yang, Z. Shao, Q. Yan, N. H. Shen, L. Shen, H. Wang, E. Li, C. M. Soukoulis, and H. Chen, "Experimental Realization of an Extreme-Parameter Omnidirectional Cloak," Research (Washington, DC, U. S.) **2019**, 1–8 (2019).

Optics EXPRESS

31. C. Zhang, J. Yang, W. Yuan, J. Zhao, J. Y. Dai, T. C. Guo, J. Liang, G. Y. Xu, Q. Cheng, and T. J. Cui, "An ultralight and thin metasurface for radar-infrared bi-stealth applications," J. Phys. D: Appl. Phys. **50**(44), 444002 (2017).
32. H. Zhang, Q. Cheng, H. Chu, O. Christogeorgos, W. Wu, and Y. Hao, "Hyperuniform disordered distribution metasurface for scattering reduction," Appl. Phys. Lett. **118**(10), 101601 (2021).
33. Z. Meng, C. Tian, C. Xu, J. Wang, X. Li, S. Huang, Q. Fan, and S. Qu, "Optically transparent coding metasurface with simultaneously low infrared emissivity and microwave scattering reduction," Opt. Express **28**(19), 27774–27784 (2020).
34. S. Zhong, L. Wu, T. Liu, J. Huang, W. Jiang, and Y. Ma, "Transparent transmission-selective radar-infrared bi-stealth structure," Opt. Express **26**(13), 16466–16476 (2018).
35. J. Li and J. B. Pendry, "Hiding under the Carpet: A New Strategy for Cloaking," Phys. Rev. Lett. **101**(20), 203901 (2008).
36. H. X. Xu, G. Hu, Y. Wang, C. Wang, M. Wang, S. Wang, Y. Huang, P. Genevet, W. Huang, and C. W. Qiu, "Polarization-insensitive 3D conformal-skin metasurface cloak," Light: Sci. Appl. **10**(1), 75 (2021).
37. C. Qian, B. Zheng, Y. Shen, L. Jing, E. Li, L. Shen, and H. Chen, "Deep-learning-enabled self-adaptive microwave cloak without human intervention," Nat. Photonics **14**(6), 383–390 (2020).
38. R. Liu, C. Ji, J. J. Mock, J. Y. Chin, T. J. Cui, and D. R. Smith, "Broadband Ground-Plane Cloak," Science **323**(5912), 366–369 (2009).
39. T. Ergin, N. Stenger, P. Brenner, J. B. Pendry, and M. Wegener, "Three-Dimensional Invisibility Cloak at Optical Wavelengths," Science **328**(5976), 337–339 (2010).
40. M. M. Sadeghi, S. Li, L. Xu, B. Hou, and H. Chen, "Transformation optics with Fabry-Pérot resonances," Sci. Rep. **5**(1), 8680 (2015).
41. Q. He, S. Xiao, X. Li, and L. Zhou, "Optic-null medium: realization and applications," Opt. Express **21**(23), 28948–28959 (2013).
42. F. Sun and S. He, "Optical Surface Transformation: Changing the optical surface by homogeneous optic-null medium at will," Sci. Rep. **5**(1), 16032 (2015).
43. A. Abdolali, H. Barati Sedeh, and M. H. Fakheri, "Geometry free materials enabled by transformation optics for enhancing the intensity of electromagnetic waves in an arbitrary domain," J. Appl. Phys. **127**(5), 054902 (2020).
44. M. H. Fakheri, A. Ashrafian, H. Barati Sedeh, and A. Abdolali, "Experimental Verification of Shape-Independent Surface Cloak Enabled by Nihility Transformation Optics," Adv. Opt. Mater. **9**(19), 2100816 (2021).
45. M. Y. Zhou, L. Xu, L. C. Zhang, J. Wu, Y. B. Li, and H. Y. Chen, "Perfect invisibility concentrator with simplified material parameters," Front. Phys. **13**(5), 134101 (2018).